Eur. Phys. J. D **9**, 323–326 (1999)

**THE EUROPEAN PHYSICAL JOURNAL D**

EDP Sciences


# Stability patterns of multiphoton ionized $YAu_n$ clusters

H. Weidele, S. Bouckaert, W. Bouwen, F. Vanhoutte, P. Lievens, and R.E. Silverans

Laboratorium voor Vaste-Stoffysica en Magnetisme, K.U. Leuven, Celestijnenlaan 200 D, B-3001 Leuven, Belgium

Received: 1 September 1998 / Received in final form: 10 November 1998

**Abstract.** Binary $Y_mAu_n$ metal clusters ($m \leq 5$, $n \leq 65$) are produced by a laser vaporization source. The clusters are ionized and excited by multiphoton absorption ($E_{h\nu} = 6.4$ eV) and mass abundance spectra were taken by time-of-flight mass spectrometry. The mass spectra of the $YAu_n$ ions reveal distinct intensity steps at $n = 2$, 6, 16, 32, and 56 which correspond for $n > 2$ to the well known electronic shell model, provided that the yttrium atom contributes three free electrons to the metallic binding of the gold clusters.

**PACS.** 36.40.Qv Stability and fragmentation of clusters – 36.40.Cg Electronic and magnetic properties of clusters

## 1 Introduction

Mass abundance spectra of simple metallic clusters, which are highly excited, reveal a stability pattern corresponding to the well known electronic shell model [1]. Such peculiar characteristics are experimentally not observed for transition metal clusters consisting of atoms with open *d*-orbitals. However, a promising way to study the electronic properties of transition metals is through binary metal clusters. Binary clusters can be successfully characterized by carefully choosing elements, where at least one of them exhibits electronic shell effects in the form of pure clusters. This restricts the choice to a simple metal, such as an alkali, a coinage metal, or aluminium [1]. The influence on the shell structure by adding transition metal atoms to these clusters can then be investigated [2–5]. On the theoretical part, transition metals are very difficult to model, since the electronic properties due to the *d*-electrons make calculations rather complex. Therefore, the description of the electronic properties of binary metal clusters concentrated so far mainly on systems exhibiting shell effects [6, 7].

The experimental study of binary metal clusters started more than a decade ago [8, 9]. These early studies were basically focused on the combination and stoichiometry of mixed alkali clusters. Extensive measurements have been performed by the group of Kaya who investigated for example the properties of clusters consisting of mono- and trivalent atoms of the main group [2, 3]. More recently, Na clusters containing a divalent metal atom have been thoroughly studied [4]. Interestingly, in many $Na_nX$ systems the well-known electronic shell effects have been observed, however for some of them, the magic numbers appear at size $n = 6$ and 16 (X = Ba, Eu), 6 and 17 (X = Br), 6 (X = Ca), and 7 (X = Mg). This is explained by a local minimum in the jellium-like background potential of the shell model due to the additional atom X which leads to an inversion of certain electronic energy levels. The ionization potentials of a more complicated system, consisting of trivalent Al clusters containing a Co atom, has also been investigated [5]. Also there, electronic shell closings and an odd-even staggering have been observed, however, these effects vanish by adding more Co atoms to the Al clusters.

In this paper, we present a study of Au clusters doped with an Y atom and investigate the stability patterns of mass abundance spectra after multiphoton ionization. Yttrium is an ideal candidate for such a study, since it is a transition metal of the IIIA group where in the atom only one electron occupies the 4-*d* orbital. Furthermore, yttrium has like gold only one isomer, which allows to resolve the abundance spectra to relatively high masses.

## 2 Experiment

We restrict the description of the experimental procedure to the generation and investigation of $YAu_n$ clusters. A thorough description of the binary cluster source will be given elsewhere [10]. Binary metal clusters are produced by a laser vaporization source. The laser vaporization technique for bimetallic cluster production, developed for metals with high boiling points, is mainly applied using dual rod sources and one or two lasers for vaporization [3, 11]. Our concept of binary cluster production is based on the application of two vaporization lasers, however, the targets of the cluster source are disks.

The principle of the source is shown in Fig. 1 and is similar to the one described recently [12]. The stainless steel source is mounted on a fast pulsed valve (R.M. Jordan) with a 15 mm thick Teflon block in between for thermal isolation during optional cooling. The sample holder

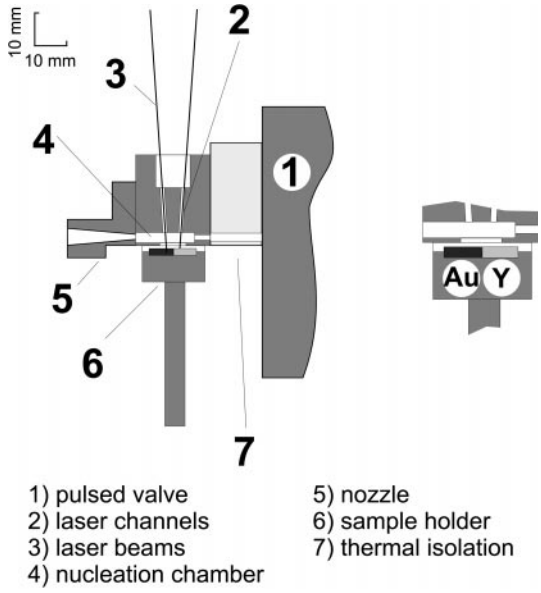


**Fig. 1.** Bimetallic laser vaporization source.

containing the targets is rectangular and moves under computer control in the $xy$-directions to prevent hole drilling from the incoming lasers. Two metal sheets of 1 mm thickness are placed next to each other, where, in the present experiment, the one next to the incoming gas pulse is yttrium (99.9% purity) and the other one is gold (99.995% purity). To prevent leakage of the incoming buffer gas the sample holder is sealed on its edges by a rectangular Teflon insert which, due to its low dynamical friction, also allows a smooth movement along the flat surface of the source.

The experimental procedure runs on a repetition rate of 10 Hz. For the production of $Y_mAu_n$ clusters, yttrium and gold are vaporized by two Nd:YAG lasers ($2^{nd}$ harmonic), where each beam is directed by a 50 cm focusing lens onto the corresponding target. Note that for optimum $YAu_n$ cluster production, special care has been taken concerning the time-delay between the two vaporization lasers ($\approx 120\,\mu$s) and the power of each laser ($\approx 15$ mJ/pulse for Y and $\approx 30$ mJ/pulse for Au). The thus created plasmas enter the formation room through a slit in the source block which allows good mixing. He gas from the pulsed valve (125 $\mu$s pulse width, 7 bar backpressure) enters the formation room of the source, cools the plasma mixture and initiates cluster production. The clusters are further cooled by expansion through a conical nozzle of 1 mm diameter into the vacuum.

The clusters pass a differential pumping stage through a skimmer and enter the acceleration stage of a reflectron time-of-flight (TOF) mass spectrometer. Neutral clusters are ionized and heated by multiphoton absorption using the laser light of an ArF-excimer laser ($E_{h\nu} = 6.4$ eV, $\approx 10\,\mathrm{mJ/cm^2}$). The ions are finally mass-selected and detected by TOF mass spectrometry [12]. The resulting mass abundance spectra are stored and analyzed on a personal computer.

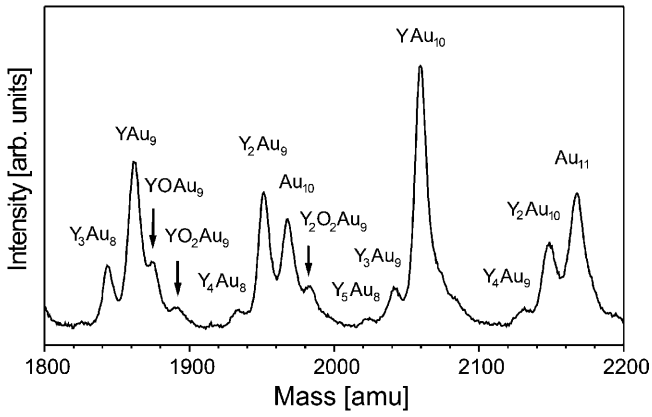


**Fig. 2.** Extraction of a mass abundance spectrum of $Y_mAu_n^+$ clusters and oxides ($m \leq 5$).

## 3 Production of $Y_mAu_n$ clusters

In Fig. 2 a small mass range of the observed abundance spectrum of mixed Y and Au clusters is shown. The combinations of clusters observed after multiphoton absorption and ionization are indicated. Clearly, the most prominent peaks are belonging to the $YAu_n^+$ clusters and to a lesser degree also pure $Au_n^+$ clusters are visible. Some smaller peaks are assigned to $Y_mAu_n^+$ clusters with $m \leq 5$. Pure yttrium clusters do not show up in the spectrum. Less prominent are oxides and dioxides of some Y−Au combinations, but oxidation of pure gold clusters is not visible. If under the same experimental conditions only yttrium is mounted as a target, then oxidized yttrium clusters are much more prominent compared to the pure yttrium clusters. This high probability for oxidation has also been seen during ionization potential measurements of $Y_n$ [13]. Indications of shell and odd-even effects are absent for yttrium clusters and their oxides in contrast to plain gold clusters. The preference for the production of binary clusters with large Au contents and some few oxides can be evaluated by comparing the dissociation energies $D_0$ of the respective dimers Y−Au (3.15 eV) > Au−Au (2.29 eV) > Y−O (1.77 eV) > Y−Y (1.65 eV) [14–16]. The higher binding energies of Y−Au and Au−Au indicate that the clusters, after the fragmentation process, contain only few combinations with Y−O and pure Y and that the number of Au atoms is by far higher. Note that this coarse approximation would also favor Y−Au combinations which would require a better mixing.

## 4 Stability patterns of $YAu_n^+$

Figure 3 represents a mass spectrum when the delay time between the two vaporization laser beams is specifically trimmed for $YAu_n^+$ and $Au_n^+$ cluster production up to size $n = 65$. The spectrum exhibits distinct reproducible stability patterns for both $YAu_n^+$ and $Au_n^+$. Intensity steps for $Au_n^+$ are observed at $n = 3$, 9, 19, (21), 35, and 59. The intensity peaks of $YAu_n^+$ are indicated by the solid line to

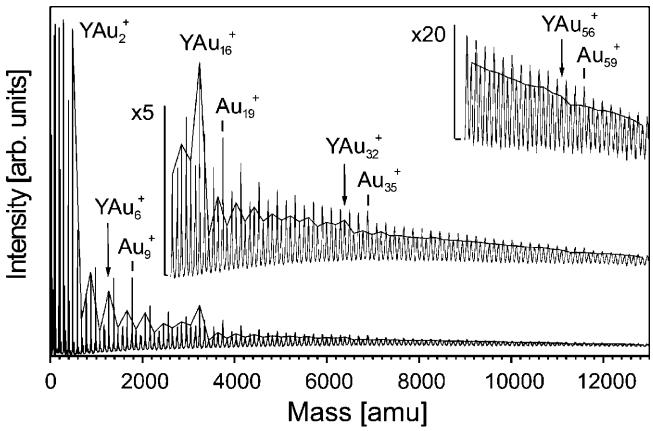


**Fig. 3.** Stability pattern of $Au_n^+$ and $YAu_n^+$ (indicated by the solid line) after multiphoton ionization.

guide the eye and very prominent peaks are observed at $n = 2$, 6, 16, 32, and 56. The pronounced patterns of $Au_n^+$ and $YAu_n^+$ in the mass abundance spectrum are a result of cooling by fragmentation. According to these magic numbers, the threshold of particle evaporation is for certain cluster sizes higher than for neighboring sizes. The high stability of these clusters can be explained by electronic shell models [1], where the magic numbers correspond to electronic shell closings at $n_e = 2$, 8, 18, (20), 34, and 58, in agreement with the filled shells: $1s$, $1p$, $1d$, $2s$, $1f$, and $(2p\ 1g)$. In these models the magic numbers are derived by considering the valence electrons of the atoms in a cluster as delocalized and confined in a smeared-out "jellium-like" ionic background potential. In general, spherical symmetric potentials are used which can be refined by taking deformations into account [1]. A second feature in the spectrum is the odd-even alternation of both $Au_n^+$ and $YAu_n^+$ clusters which can be observed up to $n \approx 40$. This is explained by the spin degeneracy of the electrons which increases the stability of the clusters through size-dependent deformations [17].

Taking a closer look to the gold cluster ions, the observations agree with those of earlier experiments [18, 19]. Gold atoms with the electronic configuration $[Xe]4f^{14}5d^{10}6s^1$ provide each one $s$-electron into the "conduction band" of a cluster. This leads for gold clusters to the magic numbers as given above which correspond to the electronic shell model for simple metallic clusters [1]. Note that one electron is removed from the clusters due to ionization. The intensity step at $n = 19$ ($n_e = 18$) is not very distinct and, as in other experiments, a small discontinuity corresponding to a filled $2s$ shell is also observed at $n = 21$ ($n_e = 20$) [18]. The step at $n = 59$ ($n_e = 58$) is rather small which can be explained by the reduced cluster ion intensity in this size range due to the cluster production and the subsequent fragmentation process.

The electronic shell closings $n_e$ for $YAu_n^+$ correspond to those of $Au_n^+$, if the Y atom provides 3 free electrons to the metallic binding of the system, with the exception of $YAu_2^+$ where only one electron is necessary. This is clarified by considering the electronic configuration of the Y atom which is $[Kr]5s^24d^1$. Obviously all three electrons above the very stable Kr-orbital of the atom (which includes the $d$-electron) are freely confined into the cluster's core potential. The high abundance of $YAu_2^+$ complies with measurements of the isoelectronic neutral YAu molecule which reveals, as shown above, a higher thermodynamic stability than neutral $Au_2$ [14, 16]. The Y and Au atom have each one valence electron which occupies the first atomic $4d$-orbital, respectively $6s$-orbital. Therefore, the $YAu_2^+$ binding must be due to two unpaired valence electrons from these atomic orbitals which form a new molecular orbital with paired electrons thus leading to a strong binding.

The intensity steps of $YAu_n^+$ at $n = 2$ ($n_e = 2$) and $n = 16$ ($n_e = 18$) are very prominent and much larger than anywhere else in the spectrum including the $Au_n^+$ clusters whereas the step at the larger size $n = 56$ ($n_e = 58$) is rather small due to the reasons given above for $Au_{59}^+$. Note that in contrast to the observation of a step at $Au_{21}^+$ for pure Au clusters, no indication for a $2s$ shell closure at $YAu_{18}^+$ is visible, which is consistent with an energy shift of the $2s$ orbital towards near-degeneracy with the $1f$ shell [20]. However, compared to $Au_9^+$ a less pronounced step is observed for $YAu_6^+$ ($n_e = 8$). This is an indication that the smaller binary clusters are strongly deformed by the addition of the Y atom. The release of three electrons from the Y atom into the "conduction band" of a cluster leaves behind a 3-fold positively charged ion in the ionic Au cage whose atoms only transfer one electron each into the band. The high positive charge of the Y atom initiates a strong polarization of the electrons to screen the surplus of positive charge. In terms of the electronic shell models this results in a local minimum in the potential well of a cluster, which has a strong effect on the energetic levels of the electronic conduction band [4, 8]. For most binary systems investigated up to now, it is assumed or calculated that the extra atom is located near the center of the cluster [4, 8]. However, the large difference of the atomic radii of both metals ($r_{Au} = 1.79$ Å, $r_Y = 2.27$ Å) [16], as well as of the ionic radii ($r_{Au}(+1) = 1.37$ Å, $r_Y(+3) = 0.893$ Å) [16] indicates possible additional distortions through geometric deformations [8].

## 5 Conclusion

Binary $Y_mAu_n$ clusters are produced by a modified laser vaporization source. Depending on the given source parameters for the production of clusters, the combinations between Y and Au were influenced within the size range $m \leq 5$ and approximately $n \leq 65$. Low Y contents reduce the presence of any cluster oxides. The mass abundance spectra of multiphoton ionized $Au_n^+$ and $YAu_n^+$ clusters reveal a stability pattern which can be described by the electronic shell model. Magic numbers for $YAu_n^+$ are observed at $n = 2$, 6, 16, 32, and 56 and for $Au_n^+$ at $n =$ 3, 9, 19, 21, 35, and 59, which correspond for the free electrons in the cluster ions to $n_e = 2$, 8, 18, 20, 34, and 58. This is in agreement with electronic shell models provided the Au atoms contribute each one $s$-electron to the metal-

lic bonds of $Au_n^+$ and $YAu_n^+$, and Y makes a contribution of three electrons from its atomic $5s^2 4d^1$ orbitals to $YAu_n^+$. $YAu_2^+$ is an exception. In this case the Y atom releases only one electron from the atomic $d$-shell to the binding. The observation of the odd-even effect up to $n \approx 40$ for both $Au_n^+$ and $YAu_n^+$ is a further evidence for their metallic characteristics.

This project is supported by the Belgian Fund for Scientific Research – Flanders (F.W.O.), by the Flemish Concerted Action (G.O.A.) Research Program, and by the Interuniversity Poles of Attraction (I.U.A.P.) Programme – Belgian State, Prime Minister's Office – Federal Office for Scientific, Technical and Cultural Affaires. H.W. is a Postdoctoral Researcher of the European Community Training and Mobility of Researchers Programme (T.M.R.). W.B. thanks the Flemish Institute for Scientific-Technological Research (I.W.T.) for financial support. P.L. is a Postdoctoral Researcher of the F.W.O.

## References

1. W.A. de Heer: Rev. Mod. Phys. **65**, 611 (1993)
2. A. Nakajima, K. Hoshino, T. Naganuma, Y. Sone, K. Kaya: J. Phys. Chem. **95**, 7061 (1991)
3. A. Nakajima, K. Hoshino, T. Sugioka, T. Naganuma, T. Taguwa, Y. Yamada, K. Watanabe, K. Kaya: J. Phys. Chem. **97**, 86 (1993)
4. C. Yeretzian: J. Phys. Chem. **99**, 123 (1995)
5. W.J.C. Menezes, M.B. Knickelbein: Z. Phys. D **26**, 322 (1993)
6. C. Baladron, J.A. Alonso: Physica B **154**, 73 (1988)
7. C. Yannouleas, P. Jena, S.N. Khanna: Phys. Rev. B **46**, 9751 (1992)
8. W.A. de Heer, W.D. Knight, M.Y. Chou, M.L. Cohen: Solid State Phys. **40**, 93 (1987)
9. M.M. Kappes, M. Schär, E. Schumacher: J. Phys. Chem. **91**, 658 (1987)
10. W. Bouwen, P. Thoen, F. Vanhoutte, S. Bouckaert, F. Despa, H. Weidele, R.E. Silverans, P. Lievens: submitted to Rev. Sci. Instrum.
11. R.L. Wagner, W.D. Vann, A.W. Castleman, Jr.: Rev. Sci. Instrum. **68**, 3010 (1997)
12. P. Lievens, P. Thoen, S. Bouckaert, W. Bouwen, E. Vandeweert, F. Vanhoutte, H. Weidele, R.E. Silverans: Z. Phys. D **42**, 231 (1997)
13. M. Knickelbein: J. Chem. Phys. **102**, 1 (1995)
14. R. Haque, M. Pelino, K.A. Gingerich: J. Chem. Phys. **73**, 4045 (1980)
15. M.D. Morse: Chem. Rev. **86**, 1049 (1986)
16. D.R. Lide (Ed.): *CRC Handbook of Chemistry and Physics* 1991-1992, 72th edn. (CRC Press, Boca Raton, Florida 1991)
17. C. Yannouleas, U. Landman: Phys. Rev. B **51**, 1902 (1995)
18. I. Katakuse, T. Ichihara, Y. Fujita, T. Matsuo, T. Sakurai, H. Matsuda: Int. J. Mass Spectrom. Ion Processes **74**, 33 (1986)
19. I. Rabin, C. Jackschath, W. Schulze: Z. Phys. D **19**, 153 (1991)
20. W. Bouwen, F. Vanhoutte, F. Despa, S. Bouckaert, S. Neuckermans, L. Theil Kuhn, H. Weidele, P. Lievens, R.E. Silverans: Chem. Phys. Lett., in press